Ground motion reduction in vibratory pile driving via axial and torsional vibrations

Tsetas, Athanasios; Tsouvalas, Apostolos; Metrikine, Andrei V.

Publication date
2023

Document Version
Final published version

Published in
Proceedings of the 29th International Congress on Sound and Vibration, 2023

29th International Congress on Sound and Vibration
The annual congress of the International Institute of Acoustics and Vibration (IIAV)
9–13 July 2023
ICSV29

Annual Congress of the International Institute of Acoustics and Vibration (IIAV)

GROUND MOTION REDUCTION IN VIBRATORY PILE DRIVING VIA AXIAL AND TORSIONAL VIBRATIONS

Athanasios Tsetas[1,*], Apostolos Tsouvalas[1] and Andrei V. Metrikine[1]

[1] *Faculty of Civil Engineering and Geosciences, Delft University of Technology, Delft, The Netherlands*

[*]Corresponding author email: A.Tsetas@tudelft.nl

In this paper, the characteristics of the induced ground motion are studied for two pile installation methods. Specifically, the classical axial vibratory driving is compared with the Gentle Driving of Piles (GDP) method, to investigate the effect of high-frequency torsional excitation in the soil response. For that purpose, a non-linear 3-D axisymmetric pile-soil interaction model - benchmarked against field data for both methods - is used to perform the numerical study. The friction redirection mechanism, that is mobilized due to the torsional excitation in GDP, leads to a different wavefield in the soil medium compared to axial vibro-driving. In the latter only SV-P wave motions are elicited, whereas torsion introduces SH wave motions as well. For the numerical study, the model is comprised by a thin cylindrical shell coupled with a linear elastic layered half-space through a history-dependent frictional interface. The Thin-Layer Method (TLM) coupled with Perfectly Matched Layers (PMLs) is employed to accurately describe the wave motion in the soil medium. Comparisons in terms of the peak particle velocities (PPVs) and soil particle trajectories showcase significant motion reduction due to redirection of the soil friction forces, which elicits high-frequency SH waves and reduces the SV-P wave motion.

Keywords: pile driving, soil dynamics, vibrations of shells, Green's functions, Harmonic Balance Method

1. Introduction

Pile driving is a major construction activity that induces appreciable ground motion, leading to potential damage of infrastructure due to excessive vibrations. For that purpose, theoretical and experimental studies have been conducted to comprehend the physics of the process and mitigate those risks [1, 2]. Customarily, the focus of such studies has been placed on construction projects in urban areas. However, in our era the environmental impact of vibrations induced by anthropogenic activities in other habitats is drawing further attention (e.g. offshore environment). To reduce the level of environmental vibrations induced by pile driving, either mitigation measures are necessary in the case of impact piling or more environmentally friendly techniques are to be employed. Vibratory pile installation is used in onshore conditions for decades, yet in offshore projects (e.g. monopile installation) impact hammering is the predominant driving method. In view of the shift towards more environmentally friendly technologies, a body of research works is focusing on various aspects of vibratory installation, e.g. drivability prediction [3], quantification of driving efficiency [4], and response to lateral loading [5].

In this paper, a numerical study is performed focusing on the ground motion induced by two pile installation methods, namely axial vibratory driving and the Gentle Driving of Piles (GDP). The latter method has been recently proposed by TU Delft and successfully demonstrated through field experiments [6, 7]. The GDP technology aims at enhancing the installation performance of axial vibro-driving through the introduction of high-frequency torsional excitation. To compare the induced ground motion by the two methods, a non-linear 3-D axisymmetric pile-soil interaction model is employed, which has been benchmarked against field data for both methods. In particular, the model is comprised by a thin cylindrical shell coupled with a linear elastic layered half-space through a history-dependent frictional interface [3]. The Thin-Layer Method (TLM) coupled with Perfectly Matched Layers (PMLs) is utilized to accurately describe the wave motion in the soil medium [8]. Comparisons in terms of velocity magnitude and soil particle trajectories showcase that the GDP method leads to significant motion reduction by redirecting the soil friction forces, thus eliciting small-wavelength SH waves and reducing the SV-P wave motion.

Figure 1: The test site of the GDP field campaign.

2. Pile-soil model of the installation process

Consider a thin cylindrical shell with wall thickness h_p, length L_p and mid-surface radius R_p. The thin shell is comprised by linear isotropic elastic material with Young's modulus E_p, Poisson ratio ν_p and mass density ρ_p. The semi-analytical finite element (SAFE) method is utilized to model the pile and the respective equations of motion according to the Love-Timoshenko shell theory read [3, 9]:

$$\mathbf{I}^{\mathrm{s}}_{\mathrm{p},0}\frac{\mathrm{d}^2\mathbf{u}^{\mathrm{s}}_{\mathrm{p},0}}{\mathrm{d}t^2}+\mathbf{L}^{\mathrm{s}}_{\mathrm{p},0}\mathbf{u}^{\mathrm{s}}_{\mathrm{p},0}=\mathbf{p}^{\mathrm{s}}_{\mathrm{p},0} \tag{1a}$$

$$\mathbf{I}^{\mathrm{a}}_{\mathrm{p},0}\frac{\mathrm{d}^2\mathbf{u}^{\mathrm{a}}_{\mathrm{p},0}}{\mathrm{d}t^2}+\mathbf{L}^{\mathrm{a}}_{\mathrm{p},0}\mathbf{u}^{\mathrm{a}}_{\mathrm{p},0}=\mathbf{p}^{\mathrm{a}}_{\mathrm{p},0} \tag{1b}$$

where $\mathbf{I}^{\mathrm{s}}_{\mathrm{p},0}$, $\mathbf{I}^{\mathrm{a}}_{\mathrm{p},0}$ are the shell mass matrices, $\mathbf{L}^{\mathrm{s}}_{\mathrm{p},0}$, $\mathbf{L}^{\mathrm{a}}_{\mathrm{p},0}$ are the shell stiffness matrices, $\mathbf{u}^{\mathrm{s}}_{\mathrm{p},0}$, $\mathbf{u}^{\mathrm{a}}_{\mathrm{p},0}$ are the displacement/rotation vectors at the nodal rings and $\mathbf{p}^{\mathrm{s}}_{\mathrm{p},0}$, $\mathbf{p}^{\mathrm{a}}_{\mathrm{p},0}$ are the vectors of consistent forces/moments

at the nodal rings. It is remarked that the latter vectors include also non-linear forces originating in the non-linear pile-soil interaction. The superscripts s and a denote the symmetric and anti-symmetric shell configurations, respectively [3]. Finally, the full pile displacements/rotation vector $\mathbf{u}_{\mathrm{p}}$ and the line load vector $\mathbf{p}_{\mathrm{p}}$, based on the premise of axisymmetric response, may be expressed as follows:

$$\mathbf{u}_{\mathrm{p}} = \begin{bmatrix} \mathbf{u}_0^{\mathrm{s}} \\ \mathbf{v}_0^{\mathrm{a}} \\ \mathbf{w}_0^{\mathrm{s}} \\ \boldsymbol{\beta}_{z,0}^{\mathrm{s}} \end{bmatrix}, \quad \mathbf{p}_{\mathrm{p}} = \frac{1}{2\pi R_{\mathrm{p}}} \begin{bmatrix} \mathbf{p}_{z0,\mathrm{p}}^{\mathrm{s}} \\ \mathbf{p}_{\theta 0,\mathrm{p}}^{\mathrm{a}} \\ \mathbf{p}_{r0,\mathrm{p}}^{\mathrm{s}} \\ \mathbf{m}_{zz0,\mathrm{p}}^{\mathrm{s}} \end{bmatrix} \tag{2}$$

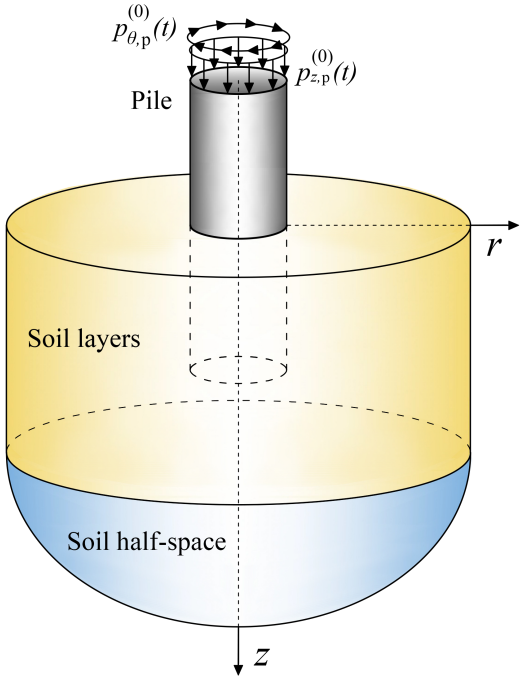

Figure 2: Installation of a pipe pile in a layered soil medium via vertical and torsional vibrations.

As regards the soil medium, a linear elastic layered half-space is considered. The computational model is based on the Thin-Layer Method (TLM) coupled with Perfectly Matched Layers (PMLs), to approximate the underlying half-space [8]. In particular, the Green's functions for unit ring sources at the pile surface are computed in the frequency-space domain [10]. Therefore, the vectors of soil displacements $\widetilde{\mathbf{u}}_{r,\mathrm{s}}$, $\widetilde{\mathbf{u}}_{\theta,\mathrm{s}}$ and $\widetilde{\mathbf{u}}_{z,\mathrm{s}}$ can be obtained in the following compact form:

$$\widetilde{\mathbf{u}}_{\mathrm{s}} = \begin{bmatrix} \widetilde{\mathbf{u}}_{r,\mathrm{s}} \\ \widetilde{\mathbf{u}}_{\theta,\mathrm{s}} \\ \widetilde{\mathbf{u}}_{z,\mathrm{s}} \end{bmatrix} = \begin{bmatrix} \widetilde{\mathbf{F}}_{rr} & \mathbf{0} & \widetilde{\mathbf{F}}_{rz} \\ \mathbf{0} & \widetilde{\mathbf{F}}_{\theta\theta} & \mathbf{0} \\ \widetilde{\mathbf{F}}_{zr} & \mathbf{0} & \widetilde{\mathbf{F}}_{zz} \end{bmatrix} \begin{bmatrix} \widetilde{\mathbf{p}}_{r,\mathrm{s}} \\ \widetilde{\mathbf{p}}_{\theta,\mathrm{s}} \\ \widetilde{\mathbf{p}}_{z,\mathrm{s}} \end{bmatrix} \tag{3}$$

where $\widetilde{\mathbf{p}}_{r,\mathrm{s}}$, $\widetilde{\mathbf{p}}_{\theta,\mathrm{s}}$, $\widetilde{\mathbf{p}}_{z,\mathrm{s}}$ denote the ring loads in the indicated directions and $\widetilde{\mathbf{F}}_{\mathrm{s}}$ is the dynamic flexibility matrix in the frequency-space domain. As can be seen, $\widetilde{\mathbf{F}}_{r\theta} = \widetilde{\mathbf{F}}_{\theta r} = \widetilde{\mathbf{F}}_{z\theta} = \widetilde{\mathbf{F}}_{\theta z} = \mathbf{0}$ due to the uncoupling of axial-radial and circumferential motions for the axisymmetric problem at hand ($n = 0$). However, the three displacement components will be coupled in the overall response due to the pile-soil friction forces, which are encompassed by the external force vector as additional loading terms. A schematic of the described model is shown in Fig. 2.

The pile-soil coupling during the installation process is realized by the following compatibility conditions:
(i) continuity of radial displacements at the pile-soil interface:

$$\mathbf{w}^{\mathrm{c}} = \mathbf{u}_r^{\mathrm{c}}\Big|_{r=R_{\mathrm{p}}} \tag{4}$$

in which the superscript c denotes the part of pile and soil along the contact interface.

(ii) compatibility of vertical tractions applied at the pile-soil interface and at the pile tip:

$$\mathbf{p}_{z,\mathrm{s}}^{\mathrm{c}} = -\mathbf{p}_{z,\mathrm{p}}^{\mathrm{c}}, \quad p_{z,\mathrm{s}}^{(\mathrm{t})} = -p_{z,\mathrm{p}}^{(\mathrm{t})} \tag{5}$$

in which the superscript (t) denotes the tip related component.

(iii) compatibility of radial tractions applied at the pile-soil interface:

$$\mathbf{p}_{r,\mathrm{s}}^{\mathrm{c}} = -\mathbf{p}_{r,\mathrm{p}}^{\mathrm{c}} \tag{6}$$

(iv) compatibility of circumferential tractions applied at the pile-soil interface:

$$\mathbf{p}_{\theta,\mathrm{s}}^{\mathrm{c}} = -\mathbf{p}_{\theta,\mathrm{p}}^{\mathrm{c}} \tag{7}$$

The Alternating Frequency-Time (AFT) Harmonic Balance Method (HBM) is employed for the solution of the coupled problem [11], with the ansatz of periodic velocity for the pile rigid body motion [12]. Further details of the numerical solution will be omitted for brevity and can be found in [3].

3. Numerical results

To compare the two methods, the respective benchmarked models are employed and the GDP piles (i.e. GDP_1 and GDP_2) from the GDP field campaign are considered [6]; the pile properties can be found in Table 1. Seismic Cone Penetration Tests with pore water pressure measurements (SCPTu) were performed to characterize the associated soil profiles (see Fig. 3). To eliminate the influence of dissimilar soil conditions for comparison purposes, the installation of vibro-driven piles is realized numerically at the locations of piles GDP_1 and GDP_2; the respective vibro-driven piles will be denoted as VH_1 and VH_2. The installation settings from the GDP field tests are used for GDP_1 and GDP_2, whereas for VH_1 and VH_2 the sole adjustment consists in using the same vibrator mass with the GDP shaker to erase any bias related to the static load. Indicatively, the driving frequencies for the cases examined are given in Table 2; more details about the driving settings can be found in [6].

ρ_{p} [kg/m^3]	E_{p} [Pa]	ν_{p} [-]	L_p [m]	R_p [m]	h_p [m]
7850	$210{\cdot}10^9$	0.3	10	0.373	0.0159

Table 1: Properties of the piles driven in the GDP field campaign.

To estimate the input load for the vibro-driven piles, a trial-and-error process is performed with the aim of achieving a fairly similar penetration profile between VH and GDP piles. In that manner, we circumvent the complication of comparing installation cases with dissimilar penetration profiles and focus solely on the induced disturbance in the soil medium. As shown in Fig. 4, the penetration profiles of VH and GDP piles can be considered similar enough to study the potential discrepancies between the elicited

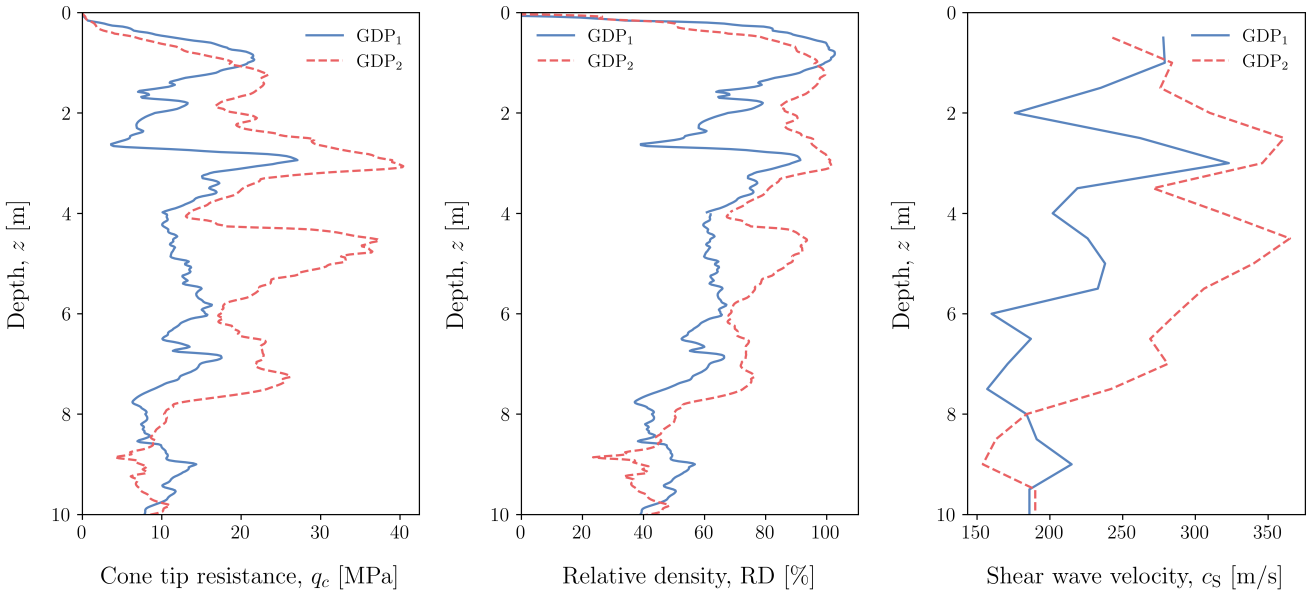

Figure 3: Profiles of (a) cone tip resistance (q_c), (b) relative density (RD), and (c) shear wave velocity (c_S) obtained from SCPTu tests.

soil motion.

		GDP_1	GDP_2	VH_1	VH_2
Axial driving frequency	f_a [Hz]	16.3	16.5	24.8	24.8
Torsional driving frequency	f_t [Hz]	62.6	63.0	-	-

Table 2: Driving frequencies for the different installation cases.

In Fig. 5, the peak particle velocities (PPVs) are compared along depth z and at three different receiver radii between the two pile installation methods. Specifically, a time window of a few cycles has been considered for VH_1 and GDP_1 piles at which the pile has penetrated 7.5 m into the soil (close to the target depth of 8 m). It is remarked that the so-called true vector sum (TVS) form of the PPV is considered. As can be seen, the PPVs are reduced in the case of GDP for all receiver radii and along the whole depth, with significant reduction with increasing receiver radius. Furthermore, in the immediate pile vicinity the largest PPVs occur in the interior soil domain and close to the tip, where the tip reaction causes a major localized disturbance. As the receiver radius increases, the largest PPVs occur along the soil surface in vibro-driving due to surface Rayleigh waves, while in GDP this occurrence cannot be distinguished. Finally, similar results have been obtained for the comparison between VH_2 and GDP_2, yet they are not reported herein due to space limitations.

To investigate further the characteristics of the induced soil motion, the ($u_{r,s}$, $u_{z,s}$) soil particle trajectories along the ground surface are visualized in Fig. 6. For both methods, in the pile vicinity the trajectories are vertically polarized and with increasing distance the retrograde elliptical orbits (typical of Rayleigh waves) are formed [13]. The particle trajectories corresponding to vibro-driving possess much higher magnitude than the ones associated with GDP. Furthermore, the obtained patterns indicate rich frequency content for GDP, which results from the coupling of the friction forces in the vertical

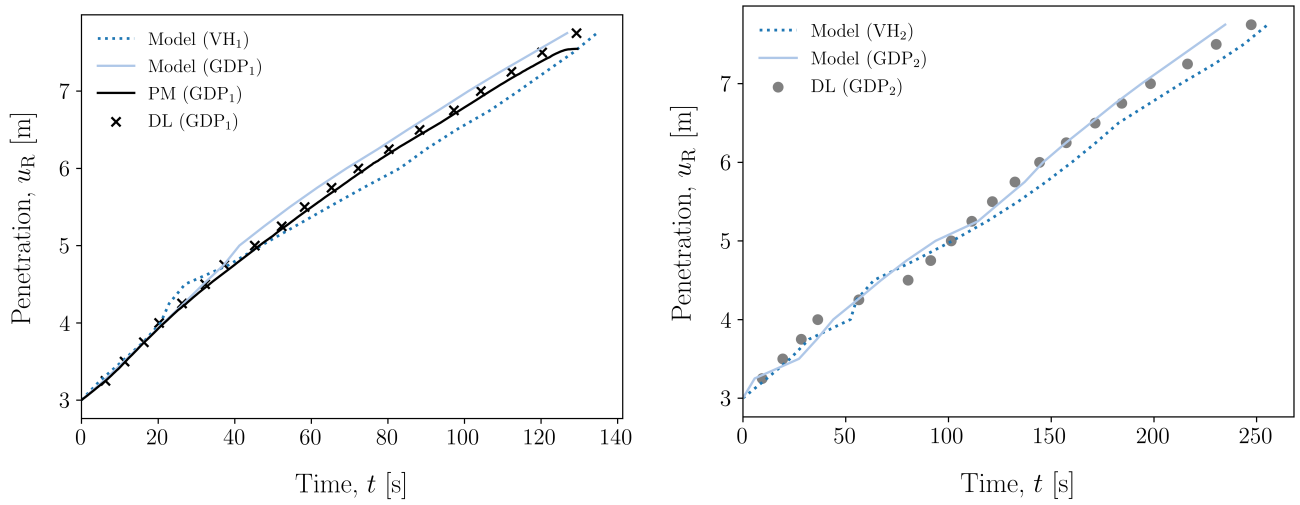

(a) GDP$_1$ location (b) GDP$_2$ location

Figure 4: Comparison of pile penetration predictions from vibratory and GDP models for the GDP$_1$ and GDP$_2$ locations; the data recorded by the potentiometer (PM) and the vibratory device logging system (DL) are also shown.

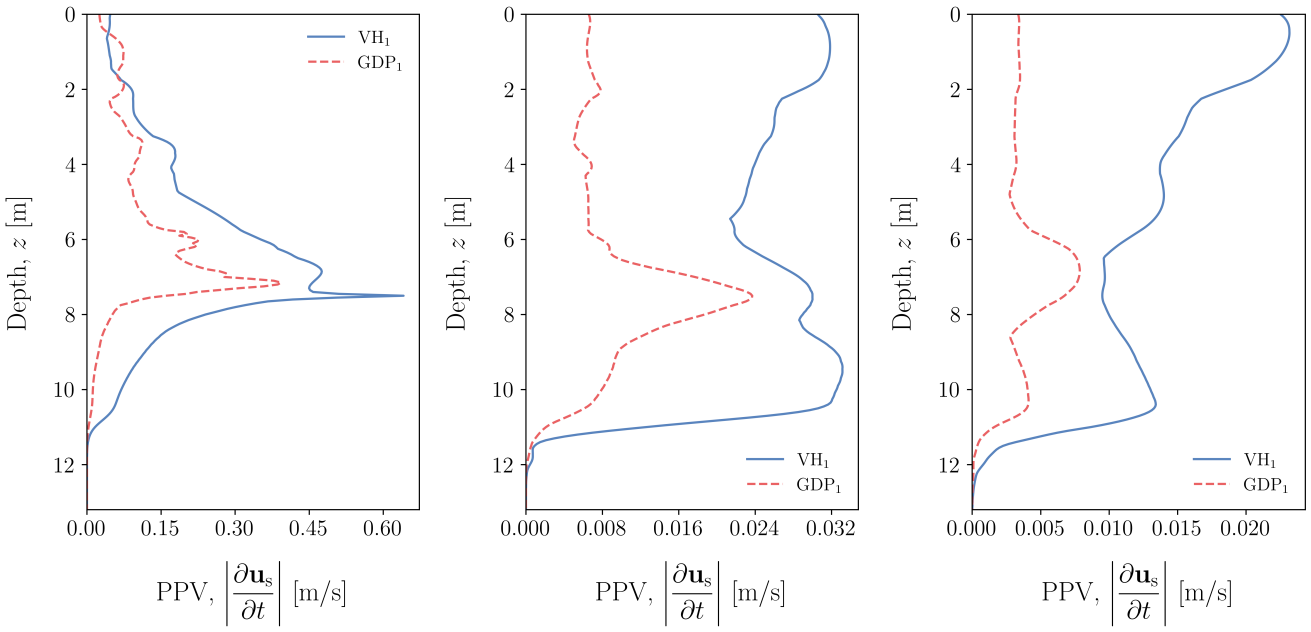

(a) (b) (c)

Figure 5: Comparison of PPVs along depth z and at receiver radius (a) $r = 0.381$ m, (b) $r = 8.40$ m, and (c) $r = 15.40$ m.

and circumferential direction and the interaction of the super-harmonics associated with the two distinct driving frequencies. Conclusively, it is interesting to note that the rate of motion decay appears higher for GDP than in axial vibro-driving as the respective orbits appear to shrink much faster with radius. The aforementioned coupling due to friction presumably shifts energy to higher frequencies which in turn dissipate faster with distance, thus leading to this rapid motion decay.

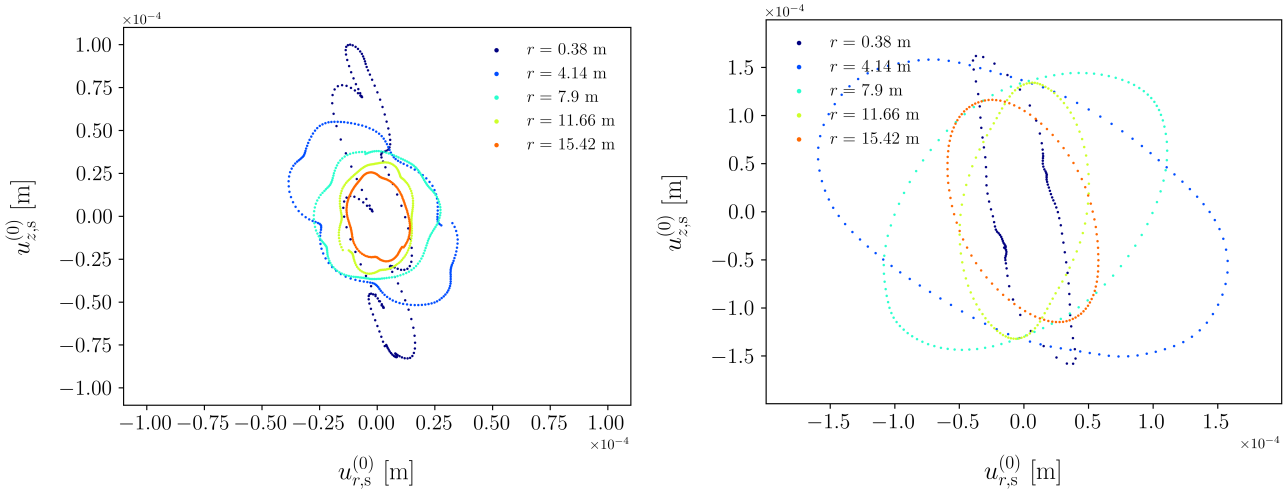

Figure 6: Trajectory of particle motion ($u_{r,\mathrm{s}}^{(0)}$, $u_{z,\mathrm{s}}^{(0)}$) at the ground surface for (a) GDP_1 and (b) VH_1.

4. Conclusions

In this paper, the ground motion induced by two different pile driving methods was studied. Specifically, the classical axial vibratory driving was compared with GDP, in order to investigate the effect of torsional vibrations at the pile head in terms of the resulting environmental disturbance. Focusing on the ground motion, the peak particle velocities both at the ground surface and in the interior soil domain were compared, as well as the soil particle trajectories. The results showcased that pile installation via GDP can lead to significantly lower magnitude of induced soil motion, which is enabled by the torsional vibrations and the coupling of vertical and circumferential friction forces. In that manner, energy is transferred into both SV-P and SH wave modes and also redistributed along the frequency spectrum, thus leading to faster motion decay.

Acknowledgments

This research is associated with the GDP project in the framework of the GROW joint research program. Funding from "Topsector Energiesubsidie van het Ministerie van Econsomische Zaken" under grant number TE-HE117100 and financial/technical support from the following partners is gratefully acknowledged: Royal Boskalis Westminster N.V., CAPE Holland B.V., Deltares, Delft Offshore Turbine B.V., Delft University of Technology, ECN, Eneco Wind B.V., IHC IQIP B.V., RWE Offshore Wind Netherlands B.V., SHL Offshore Contractors B.V., Shell Global Solutions International B.V., Sif Netherlands B.V., TNO, and Van Oord Offshore Wind Projects B.V.

REFERENCES

1. Masoumi, H. R., François, S. and Degrande, G. A non-linear coupled finite element–boundary element model for the prediction of vibrations due to vibratory and impact pile driving, *International Journal for Numerical and Analytical Methods in Geomechanics*, **33** (2), 245–274, (2009).

2. Grizi, A., Athanasopoulos-Zekkos, A. and Woods, R. D. Ground vibration measurements near im-

pact pile driving, *Journal of Geotechnical and Geoenvironmental Engineering*, **142** (8), 04016035, (2016).

3. Tsetas, A., Tsouvalas, A. and Metrikine, A. V. A non-linear three-dimensional pile–soil model for vibratory pile installation in layered media, *International Journal of Solids and Structures*, **269**, 112202, (2023).

4. Gómez, S. S., Tsetas, A. and Metrikine, A. V. Energy flux analysis for quantification of vibratory pile driving efficiency, *Journal of Sound and Vibration*, **541**, 117299, (2022).

5. Kementzetzidis, E., Pisanò, F., Tsetas, A. and Metrikine, A. Gentle Driving of Piles (GDP) at a sandy site combining axial and torsional vibrations: quantifying the influence of pile installation method on lateral behaviour, *Journal of Geoenvironmental and Geotechnical Engineering, under review*.

6. Tsetas, A., Tsouvalas, A., Gómez, S., Pisanò, F., Kementzetzidis, E., Molenkamp, T., Elkadi, A. and Metrikine, A. Gentle Driving of Piles (GDP) at a sandy site combining axial and torsional vibrations: Part I - installation tests, *Ocean Engineering*, **270**, 113453, (2023).

7. Kementzetzidis, E., Pisanò, F., Elkadi, A., Tsouvalas, A. and Metrikine, A. Gentle Driving of Piles (GDP) at a sandy site combining axial and torsional vibrations: Part II - cyclic/dynamic lateral loading tests, *Ocean Engineering*, **270**, 113452, (2023).

8. de Oliveira Barbosa, J. M., Park, J. and Kausel, E. Perfectly matched layers in the thin layer method, *Computer Methods in Applied Mechanics and Engineering*, **217**, 262–274, (2012).

9. Timoshenko, S. P. and Woinowsky-Krieger, S., *Theory of plates and shells*, McGraw-hill (1959).

10. Kausel, E. and Peek, R. Dynamic loads in the interior of a layered stratum: an explicit solution, *Bulletin of the Seismological Society of America*, **72** (5), 1459–1481, (1982).

11. Krack, M. and Gross, J., *Harmonic balance for nonlinear vibration problems*, vol. 1, Springer (2019).

12. Tsetas, A., Tsouvalas, A. and Metrikine, A. V. An alternating frequency-time harmonic balance method for fast-slow dynamical systems, *Proceedings of the 28th International Congress on Sound and Vibration*, International Institute of Acoustics and Vibration, IIAV, (2022).

13. Aki, K. and Richards, P. G., *Quantitative seismology*, University Science Books (2002).